

Rotavirus Infection Stimulates the Cl^- Reabsorption Process across the Intestinal Brush-Border Membrane of Young Rabbits

Mathie Lorrot, Sandra Martin, and Monique Vasseur*

Institut National de la Santé et de la Recherche Médicale, Unité 510, Faculté de Pharmacie, Université de Paris XI, 92296 Châtenay-Malabry, France

Received 13 March 2003/Accepted 13 June 2003

Rotavirus is a major cause of infantile gastroenteritis worldwide. However, the mechanisms underlying fluid and electrolyte secretion associated with diarrhea remain largely unknown. We investigated the hypothesis that loss of Cl^- into the luminal contents during rotavirus infection may be caused by a dysfunction in the chloride absorptive capacity across the intestinal brush-border membrane (BBM). The luminal Cl^- concentrations in the entire small intestine of young rabbits infected with lapine rotavirus decreased at 1 and 2 days postinfection (dpi), indicating net Cl^- absorption. At 7 dpi, luminal Cl^- concentrations were slightly increased, indicating a moderate net Cl^- secretion. By using a rapid filtration technique, ^{36}Cl uptake across BBM was quantified by modulating the alkali-metal ion, electrical, chloride, and/or proton gradients. Rotavirus infection caused an identical, $127\% \pm 24\%$ increase in all Cl^- uptake activities (Cl^-/H^+ symport, Cl^- conductance, and Cl^- /anion exchange) observed across the intestinal BBM. The rotavirus activating effects on the symporter started at 1 dpi and persisted up to 7 dpi. Kinetic analyses revealed that rotavirus selectively affected the capacity parameter characterizing the symporter. We report the novel observation that rotavirus infection stimulated the Cl^- reabsorption process across the intestinal BBM. We propose that the massive Cl^- reabsorption in villi could partly overwhelm chloride secretion in crypt cells, which possibly increases during rotavirus diarrhea, the resulting imbalance leading to a moderate net chloride secretion.

Rotavirus is the leading cause of infantile gastroenteritis and is responsible for high morbidity in developed countries and high mortality in developing areas of the world (8, 19). The virus infects the mature enterocytes in the upper two-thirds of villus epithelia (28, 35), and the idea is now gaining ground that diarrhea is not necessarily a consequence of any physical lesion but can precede it, as if cell dysfunction were the cause rather than the consequence of the histological damage (10, 14, 21, 28, 30).

Recently, it was shown that rotavirus impairs both Na^+ -D-glucose (SGLT1) and Na^+ -L-leucine symport activities across intestinal brush-border membrane (BBM) isolated from young rabbits (20). Because SGLT1 is known to be involved in intestinal water reabsorption under physiological conditions (26), we propose that the mechanism of rotavirus diarrhea might involve generalized inhibition of Na^+ -solute symport systems and hence of water reabsorption (20). However, rotavirus disease is known to be multifactorial (14, 28, 30), and additional mechanisms might be needed.

Rotavirus has been reported to lower intestinal disaccharidase activities both in vivo in young mice (11) and in vitro in human Caco-2 cells (25). It has been proposed that the capacity of rotavirus to increase fluid and electrolyte secretion might be attributed in part to the action of the enterotoxin NSP4 or its cleavage product, NSP4-(112-175), after it is released from virus-infected cells (14, 15, 30, 43). This peptide, which induces diarrhea in neonatal mice as did full-length NSP4 and NSP4-(114-135) peptide (4), would bind to a yet-unidentified apical

membrane receptor in villus enterocytes or crypt cells or both and would directly or indirectly trigger signal transduction pathways to enhance net chloride secretion (15, 30, 43). However, the question arises as to the physical accessibility and binding capacity of luminal enterotoxin to the cells of the crypt region (28). Thus, the cellular and molecular bases by which rotavirus infection and NSP4 induce alterations in net chloride secretion remain largely unknown (4, 28, 30).

It is widely accepted that increased luminal chloride concentrations can be due to decreased absorption in the villus cells and/or increased secretion in the crypt cells (5, 17, 18, 23). To date, however, there has been little information concerning a possible dysfunction in the chloride absorptive process in rotavirus disease. It was earlier proposed that massive loss of chloride in the stools associated with the genetic disease chloridorrhea could be due to severe malfunctioning of the intestinal BBM Cl^-/H^+ symporter (39). The nonobligatory Cl^-/H^+ symporter has previously been well characterized for both BBM and basolateral membrane (BLM) vesicles isolated from guinea pig intestine and can account for Cl^-/Cl^- exchange and Cl^- conductance activities in addition to symport of both H^+ and Cl^- (2, 3, 36, 39, 40, 42).

In the present study we investigated the hypothesis that loss of Cl^- into the luminal contents during rotavirus infection may be caused by a dysfunction in chloride transport across the intestinal BBM vesicles purified from young rabbits, which have proved to be a good animal model for studying the pathogenesis of rotavirus diarrhea (9, 20). We report the novel observation that rotavirus infection caused an identical increase in all Cl^- uptake activities (Cl^-/H^+ symport, voltage-activated Cl^- conductance, and Cl^- /anion exchange) observed across the intestinal BBM. We propose that the massive Cl^-

* Corresponding author. Mailing address: Unité 510, INSERM, Faculté de Pharmacie, Université de Paris XI, 5, rue J.-B. Clément, 92296 Châtenay-Malabry, France. Phone: (33 1) 46 83 57 96. Fax: (33 1) 46 83 58 44. E-mail: monique.vasseur@cep.u-psud.fr.

reabsorption in villi could partly overwhelm chloride secretion in crypt cells, which possibly increases during rotavirus diarrhea, the resulting imbalance leading to a moderate net chloride secretion. A preliminary account of this work has already been published (27).

MATERIALS AND METHODS

Rabbit inoculations and sample collection. Specific-pathogen-free (SPF) 4-week-old New Zealand albino hybrid rabbits were obtained from Charles River (France) and were maintained at the animal house of the University of Paris-Sud, Châtenay-Malabry, as previously described (20). Rabbits were orally inoculated with 2 ml of the lapine rotavirus stock suspension, strain La/RR510 ($10^{5.7}$ infectious particles/rabbit) (20).

At appropriate times after infection, three to seven animals were killed by cervical dislocation after stunning. For each animal, the entire contents of the small intestine were collected and then filtered to remove debris before performing measurements of ionic concentrations (ion-selective electrodes for Cl^- [ISA Biologie] and Na^+ and K^+ [Kone Optima]). Rotavirus present in the intestinal fluid of infected rabbits was quantified by enzyme immunoassay (IDEIA rotavirus test; DAKO Diagnostics, Cambridgeshire, England). For the transport study, the entire small intestine was removed, rinsed with saline at room temperature, everted, and distributed into plastic bags for storage at -80°C , as described previously (20, 39).

BBM vesicle preparation. Rabbit intestinal BBM vesicles were prepared by using the magnesium precipitation method as described previously (20, 22, 39). They were suspended at about 20 mg of membrane protein per ml in the appropriate membrane buffer (20 mM HEPES, 40 mM citric acid, 100 mM concentration of either Tris gluconate, K^+ gluconate, or KCl -0.02% LiN_3 , supplemented to a total osmolarity of 560 mOsm with sorbitol and adjusted to pH 7.5 with Tris base) and stored in liquid nitrogen until the day of transport assay, as described previously (20, 36, 37, 39, 40). All the vesicles were normal according to a series of previously defined criteria (20). Membrane protein concentrations were measured with a Bio-Rad protein assay kit, with bovine serum albumin as the standard.

Transport assay and expression of results. Chloride transport was assayed by using ^{36}Cl and a rapid filtration technique as described previously (2, 3, 36, 37, 39, 40, 42). Before use, H^{36}Cl ($0.4 \text{ mCi mmol}^{-1}$; Amersham) was neutralized with Tris base (39). Briefly, 5 μl of a BBM vesicle preparation was used to carry out uptake measurements by mixing with 45 μl of transport buffer formed by the membrane buffer supplemented with either constant or variable concentrations of unlabeled substrate (5 to 100 mM), 5 mM ^{36}Cl , and the amount of sorbitol necessary to secure a total osmolarity of 660 mOsm and was adjusted to either pH 7.5 or pH 5.0 with Tris base (final concentrations and pH in the incubation mixtures). When present, valinomycin (Sigma), a potassium specific ionophore, was dissolved in ethanol and was allowed to evaporate to dryness before being mixed with the membrane preparation (39). Initial uptake rate measurements were carried out for 4 s at 22°C (20, 39). Results are expressed as absolute velocities, v , in $\text{nanomoles} \cdot \text{seconds}^{-1} \cdot \text{milligram of protein}^{-1} \pm$ standard deviation (SD), of the pool of several experiments performed with 3 to 7 different BBM vesicle preparations. Uptake data were statistically compared by using a global F test (33).

Kinetic analyses. Uncorrected, initial absolute entry rates as a function of the substrate (*cis* Cl^-) concentration were fitted by nonlinear least-squares regression analysis to an equation containing one saturable, Michaelian transport system plus a diffusional component:

$$v = \{ [V_{\max} / (K_i + [S])] + K_d \} \cdot [S] \quad (1)$$

where V_{\max} and K_i are the capacity and affinity parameters of classic Michaelis-Menten kinetics, respectively, S is the substrate, and K_d is an apparent diffusion constant (3, 20, 36, 39). To perform each fit, the procedure of Fletcher and Powell as modified by van Melle and Robinson (38) was used. To test the fit of data to equation 1, we used the commercial program Stata (Integral Software, Paris, France). For statistical evaluation, fits were compared either within each given condition (F test) or between pairs of conditions (F' test), as described previously (3, 20, 36, 39). To determine which kinetic parameters were affected, fits were performed under the restriction of one parameter common to the two sets of data (F'' test) (38). All calculations were performed on Apple Macintosh microcomputers.

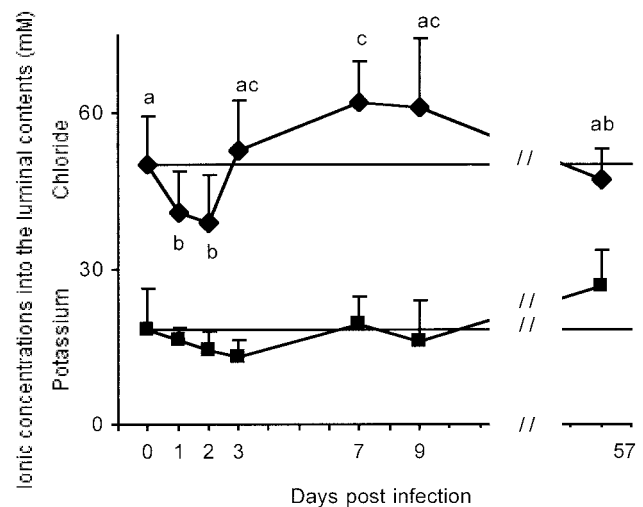


FIG. 1. Ionic concentrations in the intestinal fluid of noninfected and experimentally infected rabbits. Potassium and chloride concentrations in the luminal contents from the entire small intestine of each animal were determined as a function of time after infection. Results are expressed in millimolar \pm SD, with $n = 8$ to 43 determinations per point obtained from 4 to 12 rabbits. Because the results for four to nine noninfected rabbits at 0, 8, and 57 dpi were statistically indistinguishable, data have been pooled and are shown as a horizontal line. Identical letters indicate results found to be statistically indistinguishable according to a global F test ($P < 0.01$).

RESULTS

Ionic concentrations in the intestinal contents of noninfected and infected rabbits. Luminal K^+ concentrations were not significantly modified by rotavirus infection (Fig. 1, lower curve). Similarly, rotavirus had no effect on luminal Na^+ concentrations (data not shown). On the contrary, the Cl^- concentrations in the intestinal lumen appeared to undergo a biphasic change during the time course of infection (Fig. 1, upper curve). At 1 and 2 days postinfection (dpi), luminal Cl^- concentrations decreased significantly below control values, indicating a net Cl^- absorption. At 3 dpi, at the time of maximal virus shedding and net increase in intestinal fluid volume of infected rabbits (20), a slight increase in Cl^- concentrations was apparent. At 7 dpi, coinciding with the time of mild diarrhea (20), luminal Cl^- concentrations were significantly increased (by about 24%) compared to control values, indicating a moderate net Cl^- secretion. Thereafter, luminal Cl^- contents returned to basal level.

Evidence for pH gradient-dependent uphill transport of Cl^- across intestinal BBM from young rabbits. Considering our previous reports that an alkaline-inside pH gradient can furnish the energy necessary for the uphill transport of Cl^- across intestinal BBM and BLM purified from guinea pigs (2, 3, 36, 39, 40), we specifically looked for the presence of overshoot phenomena in BBM from young rabbits.

In the presence of a pH_o/pH_i (o [out] and i [in] indicate the extra- and intravesicular spaces, respectively) gradient of 5.0/7.5, Cl^- uptake took place uphill (Fig. 2, upper curve), yielding a fast overshoot with the characteristics of the intestinal BBM Cl^-/H^+ symporter (12, 39). When imposing an outward-directed Cl^- gradient ($[\text{Cl}^-]_o/[\text{Cl}^-]_i = 15/100 \text{ mM}$), cold *trans*

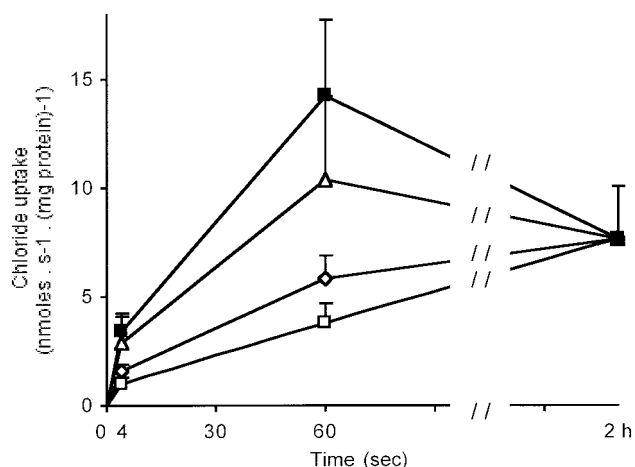


FIG. 2. Time course of chloride uptake by intestinal BBM purified from noninfected rabbits: effect of H⁺, electrical, and/or Cl⁻ gradients. Cl⁻ uptake was determined with 15 mM *cis* ³⁶Cl as substrate. The extra- and intravesicular spaces contained a 20 mM HEPES-40 mM citric acid buffer adjusted with Tris base to give at zero time a pH_o/pH_i gradient of either 7.5/7.5 (□, ◇, Δ) or 5.0/7.5 (■) and was supplemented with appropriate mixtures of either Tris gluconate, K⁺ gluconate, or KCl to obtain the following ionic concentration gradients: [K⁺]_o/[K⁺]_i = 0/0 mM and [Cl⁻]_o/[Cl⁻]_i = 15/0 mM (■, □); [K⁺]_o/[K⁺]_i = 100/0 mM and [Cl⁻]_o/[Cl⁻]_i = 15/0 mM (◇); and [K⁺]_o/[K⁺]_i = 100/100 mM and [Cl⁻]_o/[Cl⁻]_i = 15/100 mM (Δ). When K⁺ was present, valinomycin was added at 10 μg · mg protein⁻¹. Results are expressed as absolute uptake values in nanomoles · milligrams of protein⁻¹ ± SD, with *n* = 16 to 26 determinations per point derived from four different membrane preparations. Because the uptake values at equilibrium (2 h) were identical, data have been pooled (*n* = 18). So as not to overload the figure, the uptake values at 4 s, 60 s, and equilibrium were used.

Cl⁻ induced overshoots both in the absence of a pH gradient (Fig. 2, curve Δ) and in its presence (pH_o/pH_i = 5.0/7.5; data not shown), a result indicating the existence of Cl⁻/Cl⁻ exchange activity in rabbit BBM (39, 42). In contrast, no Cl⁻

overshoot was ever observed under equilibrated pH conditions (pH_o/pH_i = 7.5/7.5) in the absence or presence of alkali-metal ions (either K⁺, Na⁺, or K⁺ plus Na⁺) and electrical gradients (Fig. 2, the two lower curves), indicating the absence of any Cl⁻/Na⁺, Cl⁻/K⁺, and/or 2 Cl⁻/Na⁺/K⁺ symporter.

Total initial Cl⁻ uptake involves Cl⁻/H⁺ symport, rheogenic Cl⁻ conductance, and Cl⁻ anion exchange activities across noninfected rabbit intestinal BBM. To further investigate the mechanism(s) underlying the pH gradient-dependent uphill transport of Cl⁻ evidenced in rabbit intestinal BBM, the initial Cl⁻ entry rates were quantified in a diversity of experimental conditions aimed at modifying the alkali-metal ion, electrical, and/or Cl⁻ gradients, both in the absence and presence of an alkaline-inside pH gradient (Table 1).

Evidence for a Cl⁻/H⁺ symporter. In the complete absence of alkali-metal ions, a 2.5-unit pH gradient caused a significant increase in the initial Cl⁻ entry rate, confirming the presence of a Cl⁻/H⁺ symporter (Table 1, condition F versus A). To test whether the activation of Cl⁻ uptake by an alkaline-inside pH gradient was either electrical (rheogenic) or electroneutral, we tested the effect of short circuiting the membrane potential with 100 mM equilibrated K⁺ concentrations and valinomycin. In these conditions, voltage clamping had a small but insignificant effect on the initial influx rate (Table 1, condition I), indicating that the uphill Cl⁻ uptake driven by a pH gradient involved mainly an electroneutral Cl⁻/H⁺ symporter. In the absence of a pH gradient, the initial Cl⁻ entry rate (Table 1, condition D), which was quantitatively identical to that obtained in the complete absence of alkali-metal ions (Table 1, condition A), could be taken as the reference of basal, initial Cl⁻ entry rate in rabbit BBM.

Evidence for rheogenic Cl⁻ conductance. To further assess the contribution to total Cl⁻ uptake of a possible potential-sensitive conductance pathway, we studied the effect of valinomycin in the presence of an inward-directed K⁺ gradient ([K⁺]_o/[K⁺]_i = 100/0 mM), both with and without an alkaline-inside, 2.5-unit pH gradient. Both in the absence and in the

TABLE 1. Chloride uptake by intestinal BBM purified from noninfected controls and infected rabbits at 3 dpi: effect of potassium, electrical, and/or chloride gradients on the initial Cl⁻ entry rates in the absence and presence of a pH gradient^a

Condition and pH gradient	[K ⁺] _o /[K ⁺] _i (mM)	Val	[Cl ⁻] _o /[Cl ⁻] _i (mM)	Chlorine uptake (<i>n</i>) at dpi:		% Activation
				0	3	
7.5/7.5						
A	0/0	-	15/0	239 ± 40 (19) ab	617 ± 218 (9) de	158
B	100/0	-	15/0	295 ± 88 (41) b*	731 ± 234 (9) def	148
C	100/0	+	15/0	394 ± 84 (16) c	743 ± 219 (14) def	89
D	100/100	+	15/0	237 ± 79 (26) a	584 ± 287 (19) cd	146
E	100/100	+	15/100	725 ± 337 (24) def	1,637 ± 785 (19) g	126
5.0/7.5						
F	0/0	-	15/0	762 ± 235 (21) def	1,511 ± 239 (30) g	98
G	100/0	-	15/0	835 ± 290 (38) ef*	1,914 ± 524 (9) g	129
H	100/0	+	15/0	857 ± 164 (18) f	1,750 ± 617 (14) g	104
I	100/100	+	15/0	603 ± 230 (22) d	1,526 ± 716 (18) g	153
J	100/100	+	15/100	1,345 ± 635 (26) g	2,954 ± 1,047 (37) h	120

^a The extra- and intravesicular spaces contained a 20 mM HEPES-40 mM citric acid buffer and the indicated K⁺, electrical, and Cl⁻ gradients with pH gradients (pH_o/pH_i) of 7.5/7.5 or 5.0/7.5. Valinomycin (Val) was at 10 μg · mg of protein⁻¹. Positive-inside (conditions C and H) or short circuited to zero (conditions D, E, I, and J) membrane potentials were obtained with valinomycin and the indicated K⁺ gradients. The initial chloride entry rates, with 15 mM *cis* ³⁶Cl as substrate, are given in picomoles · milligrams of protein⁻¹ · second⁻¹ ± SD with *n* determinations per point derived from four different membrane preparations from either noninfected controls or infected animals at 3 dpi. Identical letters indicate results found to be statistically indistinguishable according to a global F test (*P* < 0.01). The asterisk means that the results obtained in the presence of 100 mM *cis* of either K⁺, Na⁺, or an equimolar mixture of Na⁺ plus K⁺ are statistically identical and have been pooled. Overall mean percent activation was 127% ± 24%.

presence of such a pH gradient, *cis* K⁺ caused small increases in the initial Cl⁻ entry rate, further increased when valinomycin was added (Table 1, conditions B, C versus D and G, and H versus I). All of these increases were abolished when the membrane potential was short circuited to zero (Table 1, conditions D and I). These results can be interpreted as being due to the stimulation of a Cl⁻ conductance pathway by the positive-inside membrane potential created by the inward-directed K⁺ gradient plus valinomycin (36, 37, 42). When alone, K⁺ had by itself just a slight electrical effect, indicating that rabbit BBM had a low intrinsic permeability for this ion. The results in Table 1 further confirm the absence of any electroneutral Cl⁻/Na⁺, Cl⁻/K⁺, or 2 Cl⁻/Na⁺/K⁺ symporter in our rabbit BBM preparations. The observation that the activations caused by 100 mM *cis* of either K⁺, Na⁺, or an equimolar mixture of Na⁺ plus K⁺ on Cl⁻ uptake were identical and fully abolished under voltage clamping conditions (Table 1, condition B versus D) indicated that the ion effects were purely electrical.

Evidence for electroneutral Cl⁻/Cl⁻ exchange activity. Cl⁻/Cl⁻ and Cl⁻/HCO₃⁻ exchange activities have both been reported to be present in enterocyte membranes of several animal species, including rat, guinea pig, and rabbit (12, 24, 31, 40, 42). Accordingly, we investigated the effects on ³⁶Cl⁻ uptake of imposing gradients of either chloride, pH, or both together in the presence of short-circuiting conditions to assess an electroneutral mechanism. Table 1 gives the results obtained by using a combination of four different, meaningful situations (conditions D, E and I, J). Both in the absence of a pH gradient and in its presence, cold *trans* Cl⁻ significantly increased the initial Cl⁻ influx. These results provide evidence for the coexistence in the same vesicles of Cl⁻/Cl⁻ exchange activity which is activated by *cis* H⁺ and a Cl⁻/H⁺ symporter which is stimulated by *trans* chloride. Similar activation of proton-gradient-driven Cl⁻ uptake by *trans* bicarbonate has also been reported in both villus and crypt cell BBM from rabbit intestine (12).

From the whole set of results, we conclude that total initial Cl⁻ uptake in rabbit intestinal BBM vesicles occurred with three distinct activities: proton-coupled Cl⁻ transport, voltage-activated Cl⁻ conductance, and Cl⁻/anion exchange.

Activating effect of rotavirus infection on Cl⁻ transport across intestinal BBM. To establish whether or not Cl⁻ uptake activities were affected in the course of rotavirus infection, Cl⁻ transport was studied by using BBM from infected rabbits. In support of earlier observations (20), virus shedding into the intestinal fluid of infected rabbits peaked at 3 dpi (data not shown). We previously reported that, at this time, significant inhibition of both SGLT1 and Na⁺-L-leucine symport activities was observed in the absence of any apparent histological damage (see Table 2 in reference 20). We therefore undertook to determine intestinal Cl⁻ transport at 3 dpi. Chloride uptake experiments were repeated in the absence or presence of K⁺, electrical, and/or Cl⁻ gradients, with or without a pH gradient.

In all the study conditions, rotavirus infection had a general activating effect on Cl⁻ uptake activities observed across the rabbit intestinal BBM (Table 1). The increases in the initial Cl⁻ entry rates were about the same (overall mean of 127% ± 24%) irrespective of the imposed gradient, suggesting that the quantitative participation of any of the activities to total initial Cl⁻ uptake could be expected to be unaffected by rotavirus infection.

TABLE 2. Quantification of rheogenic Cl⁻ conductance, Cl⁻/Cl⁻ exchange, and Cl⁻/H⁺ symport activities by intestinal BBM vesicles purified from noninfected controls and experimentally infected rabbits^a

Effect	Conditions	Uptake increments (pmol ⁻¹ · mg protein ⁻¹ · s ⁻¹) at dpi:	
		0	3
Electrical	C-D	157 (16%)	159 (7%)
<i>trans</i> chloride	E-D	488 (48%)	1053 (49%)
Proton	I-D	366 (36%)	942 (44%)

^a Conditions are as defined in footnote a of Table 1. The data are given in terms of uptake increments obtained by the difference between the reference, basal, initial Cl⁻ entry rate. The quantitative contribution of any of the activities to the total initial Cl⁻ uptake is given in parentheses.

All Cl⁻ uptake values at 1 min were slightly activated, but no Cl⁻ overshoot was ever observed under equilibrated pH conditions in the absence or presence of a K⁺ gradient with or without valinomycin (data not shown). The Cl⁻ uptake values at equilibrium (2 h) remained constant (7.52 ± 3.07 nmol · mg of protein⁻¹; n = 18) and were identical to those found for noninfected rabbits (7.84 ± 1.55 nmol · mg of protein⁻¹; n = 18; see Fig. 1), a result indicating that the apparent vesicular volume, which can be interpreted as a measure of the functional vesicle yield (6, 41), did not change during rotavirus infection. Similar conclusions were reached when studying the effect of rotavirus infection on intestinal BBM Na⁺-solute symport activities in young rabbits (20).

Quantification of Cl⁻/H⁺ symport, rheogenic Cl⁻ conductance, and Cl⁻/Cl⁻ exchange activities by intestinal BBM from noninfected and infected rabbits. Having established that initial Cl⁻ influx into BBM occurred with three different properties, Cl⁻/H⁺ symport, rheogenic Cl⁻ conductance, and Cl⁻/anion exchange, we next evaluated the quantitative participation of each activity. Among the many experimental conditions used, we selected those that would enable these calculations to be made. The relevant results are listed in Table 2, where the effects of electrical, *trans* chloride, and proton gradients were calculated in terms of the uptake increments. Taken as a whole, our results indicate that rotavirus infection did not markedly modify the proportion of either activity. About 10 and 90% of total initial Cl⁻ uptake involved electrical and electroneutral mechanism(s), respectively. Although infection appeared to abolish the voltage-activated Cl⁻ conductance activity (Table 1, condition C), the presence of this weakly operative component does not affect the general conclusion that Cl⁻/anion exchange and Cl⁻/H⁺ symport activities participated to a great extent (on average, 49 and 40%, respectively) to total Cl⁻ influx, both in infected and control BBM.

Evolution with time of proton-coupled Cl⁻ uptake by intestinal BBM from infected rabbits. To further confirm that rotavirus infection activated Cl⁻ transport, the proton-gradient-driven Cl⁻ uptake was studied as a function of time after infection. As illustrated in Fig. 3, all proton-coupled Cl⁻ uptakes across BBM from infected animals were statistically different from that of the control group. Strong activation of Cl⁻/H⁺ symport activity occurred at times as short as 1 dpi and persisted up to 7 dpi. The increases remained practically identical during the first 2 days after infection, about 132 and 109%,

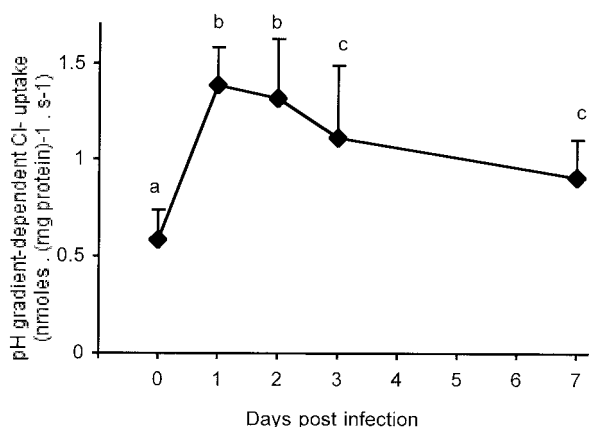


FIG. 3. Rotavirus activating effects on BBM Cl⁻/H⁺ symporter as a function of time after infection. The initial Cl⁻ entry rates were determined with 15 mM *cis* ³⁶Cl. The extra- and intravesicular spaces contained a 20 mM HEPES–40 mM citric acid–100 mM Tris gluconate buffer adjusted with Tris base to give an initial pH_o/pH_i gradient of 5.0/7.5. Results are expressed in nanomoles · milligrams of protein⁻¹ · second⁻¹ ± SD, with *n* = 18 to 72 determinations per point obtained from three to seven different membrane preparations. Identical letters indicate results found to be statistically indistinguishable according to a global F test (*P* < 0.01).

respectively. Thereafter, at 3 and 7 dpi there seemed to be a progressive fall in Cl⁻/H⁺ symport activity, although the increases were still considerable, 91 and 56%, respectively. From the whole set of observations, we conclude that rotavirus infection strongly enhanced chloride influx across rabbit BBM.

Effect of rotavirus infection on the kinetics of pH gradient-dependent Cl⁻ uptake by BBM. To understand the mechanisms involved in activation of intestinal Cl⁻ transport during rotavirus infection, kinetic analyses were performed as a function of *cis* chloride concentration in the presence of a pH gradient (pH_o/pH_i = 5.0/7.5). As previously established with intestinal BBM and BLM from guinea pigs (3, 36), the kinetics of Cl⁻ uptake in the presence of an alkaline-inside pH gradient can be described by an equation involving one Michaelian, concave hyperbola plus one linear, nonsaturable, diffusion-like component (equation 1). The values for different groups of infected animals were all statistically different from those of the control group (Table 3). The effects were highly significant at 3 dpi according to the F' test at *P* < 0.01. At 7 dpi a significant difference was apparent when the limits of probability were increased to *P* < 0.05, agreeing with the data on increased Cl⁻ uptake during rotavirus infection (Fig. 3). Also in agreement with the data shown in Fig. 3, no significant difference according to an F' test was revealed between infected rabbits at 3 and 7 dpi. Therefore, the relevant data were pooled and are shown as an overall fit (3 plus 7) in Table 3. To determine which kinetic parameters were indeed affected, the two sets of data at zero and 3 plus 7 dpi were fitted again under the restriction of one parameter common to the two sets. The F'' test revealed a significant loss of information with a common *V*_{max}, meaning that the parameter in question differed from one set to another. We conclude, therefore, that *V*_{max} was the only parameter systematically increased by rotavirus infection. In contrast, *K_t* remained practically unchanged, exhibiting

TABLE 3. Kinetics of pH gradient-dependent Cl⁻ uptake by intestinal BBM purified from noninfected controls and infected animals at 3 and 7 dpi^a

Type of examination and dpi	Kinetic parameter		F test				
	<i>V</i> _{max} (nmol · mg protein ⁻¹ · s ⁻¹)	<i>K_t</i> (mM)	F	F'	F''	df	<i>P</i>
Uptake							
0	1.76 ± 0.14	42.2 ± 5.3	0.18			[10, 204]	NS
3	2.49 ± 0.13	34.6 ± 2.9	0.49			[10, 232]	NS
7	2.17 ± 0.27	29.6 ± 5.9	0.38			[10, 41]	NS
3 + 7	2.44 ± 0.12	33.7 ± 2.6	0.36			[10, 285]	NS
Curve comparison							
0 versus 3				139		[2, 456]	HS
0 versus 7				37		[2, 265]	S
3 versus 7				0.94		[2, 293]	NS
0 versus 3 + 7				145		[2, 509]	HS
Test to determine which parameters were affected							
0 versus 3 + 7							
Common <i>V</i> _{max} at control values of 1.76					2.34	[22, 489]	HS
Common <i>K_t</i> at control values of 42					0.52	[22, 489]	NS

^a Cl⁻ saturation curves were performed by using 0 *trans*, *cis* Cl⁻ concentration in the range of 5 to 100 mM. Both the extra- and intravesicular spaces contained a 20 mM HEPES–40 mM citric acid–100 mM Tris gluconate buffer adjusted with Tris base to give an initial pH_o/pH_i gradient of 5.0/7.5. Kinetic parameters (means ± SD) were estimated by non linear regression analysis to equation 1. The kinetic diffusion constant, *K_d*, was fixed to the common value of 5 nl · mg protein⁻¹ · s⁻¹ before running each iteration (2, 3). Each set of data represents the overall fit obtained by pooling seven to eight saturation curves for four animals, except for data at 7 dpi representing two saturation curves for two animals. For the F test, the degrees of freedom (df) for pure error and lack of fit, in that order, are indicated in brackets. *P* = NS (not significant to *P* < 0.01) means that, for each given curve, the data points do not differ statistically from the theoretical fit of the equation under study. For the F' test, the results were further compared by pairs where HS and S indicate that the two curves differ significantly from one another at *P* < 0.01 and *P* < 0.05, respectively. Because the results for the rabbits infected at 3 and 7 dpi are statistically homogeneous, the relevant data have been pooled and fitted again to yield the indicated overall fit values. For the F'' test, the two sets of data at 0 and (3 and 7) dpi were fitted again under the restriction of one parameter common to the two sets. *P* = HS (significant to *P* < 0.01) reveals a significant loss of information with one common parameter shared by the two sets, meaning that the parameter in question differs from one set to another. Further details are given in the text.

a relatively high value, about 35 mM, compared to 10 mM for guinea pig BBM (3, 39, 40).

DISCUSSION

We report the novel observation that infection of young rabbits by lapine rotavirus, La/RR510 strain, caused a strong, identical increase in all Cl^- transport systems observed across intestinal BBM. Both in infected and control BBM, the rheogenic Cl^- conductance activity was weakly operative, whereas the electroneutral systems predominated: Cl^- /anion exchange and Cl^-/H^+ symport activities represented, on average, 49 and 40%, respectively, of the total initial Cl^- influx. Incidentally, such parallel increases in all three Cl^- uptake activities, caused by rotavirus infection, would appear to strengthen the concept of the same transport entity, namely a single, mobile carrier acting as a nonobligatory Cl^-/H^+ symporter (2, 3, 36, 39, 40, 42). As previously established with intestinal BBM and BLM from guinea pigs and similar to the present BBM results, external protons activated Cl^-/Cl^- exchange (Table 1, conditions E and J), a result providing evidence for the functioning of a symporter (3). In contrast, proton inhibition would be expected for an antiporter (exchanger) (3), as was the case for the erythrocyte $\text{Cl}^-/\text{HCO}_3^-$ exchanger mediated by anion exchanger AE1 (29). Taken as a whole, whether three distinct transport mechanisms or a single one was involved does not affect the general conclusion that rotavirus infection enhanced Cl^- transport across rabbit villus cell BBM.

The molecular identities of the proteins that mediate the anion exchange functions remain unknown (1, 32). Whereas AE1 appears to code for a $\text{Cl}^-/\text{HCO}_3^-$ exchanger, it has yet to be established whether or not the intestinal AE2 codes for a Cl^-/OH^- antiporter or a Cl^-/H^+ symporter (3). AE2 was first localized in rabbit ileum BBM (7) and then in BBM of both jejunum and ileum of the guinea pig and rabbit (36). More recently, AE2 was detected in both BBM and BLM of villus enterocytes and crypt cells from mice when using antibody to AE2 amino acids 109 to 122 (1). However, when using antibody to amino acids 1224 to 1237, AE2 was present in ileal BLM and not in BBM of rabbits and mice (1, 32), further confusing AE2 localization. Nevertheless, it has been speculated that AE2a is the main isoform present in the intestinal BBM (32). To date, practically nothing is known about the localization and physiological significance of the AE2 isoforms throughout the gut.

To explain a selective rotavirus effect on the V_{\max} parameter characterizing the Cl^-/H^+ symporter, two mechanisms can be envisaged, namely an increase in transporter numbers or a rise in the transporter turnover rate (20). Such mechanisms could not be demonstrated in the present paper, mainly because of practical problems of availability and specificity of antibodies to AE2 (32). Nevertheless, the fact that the Cl^- uptake values at equilibrium that provide a measure of the effective transport capacity of a given vesicle population (6, 20, 40, 41) were the same in control and infected rabbits strongly suggests that turnover rate could be the parameter affected by rotavirus infection. A similar mechanism has been proposed to explain glucose malabsorption resulting from rotavirus infection, although here infection reduced the V_{\max} parameter characterizing SGLT1 without affecting the density of phlorizin-binding

sites and the SGLT1 protein antigen present in the BBM preparations (20).

The present results indicate a biphasic change in the luminal Cl^- concentrations (Fig. 1): net Cl^- absorption at the earliest times after rotavirus infection and net Cl^- secretion at a late stage of infection, coinciding with the appearance of mild diarrhea (20). However, the increase in luminal Cl^- concentrations was found to be moderate, which would seem to be in line with observations that the ionic concentrations in the stools of rotavirus-positive children are much lower than those occurring in the secretory diarrheas caused by secretagogues, such as the enterotoxins of *Vibrio cholerae* and *Escherichia coli* (21). Davidson et al. (13) reported that net Na^+ and Cl^- fluxes in jejunal epithelium from piglets infected with human rotavirus did not differ from those in noninfected animals. Conversely, Starkey et al. (34), by using an in vitro perfusion technique and intestinal segments, showed that Cl^- transport exhibited secretion at 3 dpi, a time at which Cl^- concentrations in the luminal contents from neonatal mice were maximally elevated. They predicted that increased net Cl^- secretion could not be due to loss of chloride absorption but rather to the presence of a secretory component. However, the authors did not provide any experimental evidence for this suggestion.

We show for the first time that rotavirus infection caused no chloride malabsorption but rather activation of the absorptive capacity of Cl^- . In principle, activation of Cl^- uptake that persisted up to 7 dpi would result in net absorption, fully agreeing with our data in the first two days after infection (Fig. 1). However, this result appears to be incompatible with the slight increase in net Cl^- secretion at a late stage of infection. We propose that the massive Cl^- reabsorption in villi could overwhelm chloride secretion in crypt cells, which possibly increases during rotavirus diarrhea, the resulting imbalance leading to a moderate net chloride secretion. It should be noted that our BBM preparations were derived mostly from enterocytes (20, 37), which leaves open the question of the rotavirus effect on the Cl^- transport systems present in crypt cell BBM (12). The extent to which rotavirus can modify Cl^- transport in small-intestine crypt cells remains unknown and will be dealt with elsewhere.

Taken as a whole, the substantial chloride reabsorption reported in the present paper and the massive loss of water due to inhibition of Na^+ -solute symport systems (20) may be determining mechanisms (but not necessarily the only ones) in the watery diarrheas caused by rotavirus. Although oral rehydration solution appears to be safe and effective in all forms of acute diarrhea in childhood, progress in the understanding of intestinal pathophysiology may lead to the development of new drugs to treat the clinically important disease caused by rotavirus worldwide (16).

ACKNOWLEDGMENTS

We thank Sylvie Guérin (Paris, France) for help in performing measurements of ionic concentrations and our colleagues Raymonde Amsellem, Marie-Hélène Coconnier-Polter, and Vanessa Liévin-Le Moal for assistance with rabbit inoculations and sample collection. We also thank Guy van Melle for help with statistical analysis and Sheila Carrodus for help preparing the manuscript.

This work was supported in part by the Institut National de la Santé et de la Recherche Médicale (INSERM); by the Fondation pour la Recherche Médicale, Paris; by the Association Française de Lutte

contre la Mucoviscidose (AFLM); by the INCO Program of the European Economic Community (grant ERB 3514 PL 950019); and by the Ministère Français de l'Éducation nationale, de la Recherche et de la Technologie (grant MENRT-PRFMMIP).

REFERENCES

- Alper, S. L., H. Rossmann, S. Wilhelm, A. K. Stuart-Tilley, B. E. Shmukler, and U. Seidler. 1999. Expression of AE2 anion exchanger in mouse intestine. *Am. J. Physiol.* **277**:G321–G332.
- Alvarado, F., and M. Vasseur. 1998. Direct inhibitory effect of CCCP on the Cl⁻/H⁺ symporter of the guinea pig ileal brush-border membrane. *Am. J. Physiol.* **274**:C481–C491.
- Alvarado, F., and M. Vasseur. 1996. Theoretical and experimental discrimination between Cl⁻/H⁺ symporters and Cl⁻/OH⁻ antiporters. *Am. J. Physiol.* **271**:C1612–C1628.
- Ball, J. M., P. Tian, C. Q. Zeng, A. P. Morris, and M. K. Estes. 1996. Age-dependent diarrhea induced by a rotaviral nonstructural glycoprotein. *Science* **272**:101–104.
- Barrett, K. E., and S. J. Keely. 2000. Chloride secretion by the intestinal epithelium: molecular basis and regulatory aspects. *Annu. Rev. Physiol.* **62**:535–572.
- Brot-Laroche, E., and F. Alvarado. 1984. Disaccharide uptake by brush-border membrane vesicles lacking the corresponding hydrolases. *Biochim. Biophys. Acta* **775**:175–181.
- Chow, A., J. W. Dobbins, P. S. Aronson, and P. Igarashi. 1992. cDNA cloning and localization of a band 3-related protein from ileum. *Am. J. Physiol.* **263**:G345–G352.
- Ciarlet, M., and M. K. Estes. 2001. Interactions between rotavirus and gastrointestinal cells. *Curr. Opin. Microbiol.* **4**:435–441.
- Ciarlet, M., M. K. Estes, C. Barone, R. F. Ramig, and M. E. Conner. 1998. Analysis of host range restriction determinants in the rabbit model: comparison of homologous and heterologous rotavirus infections. *J. Virol.* **72**:2341–2351.
- Ciarlet, M., M. A. Gilger, C. Barone, M. McArthur, M. K. Estes, and M. E. Conner. 1998. Rotavirus disease, but not infection and development of intestinal histopathological lesions, is age restricted in rabbits. *Virology* **251**:343–360.
- Collins, J., D. C. Candy, W. G. Starkey, A. J. Spencer, M. P. Osborne, and J. Stephen. 1990. Disaccharidase activities in small intestine of rotavirus-infected suckling mice: a histochemical study. *J. Pediatr. Gastroenterol. Nutr.* **11**:395–403.
- Coon, S., and U. Sundaram. 2000. Mechanism of glucocorticoid-mediated reversal of inhibition of Cl⁻/HCO₃⁻(3) exchange during chronic ileitis. *Am. J. Physiol. Gastrointest. Liver Physiol.* **278**:G570–G577.
- Davidson, G. P., D. G. Gall, M. Petric, D. G. Butler, and J. R. Hamilton. 1977. Hum. rotavirus enteritis induced in conventional piglets. Intestinal structure and transport. *J. Clin. Investig.* **60**:1402–1409.
- Estes, M. K., G. Kang, C. Q. Zeng, S. E. Crawford, and M. Ciarlet. 2001. Pathogenesis of rotavirus gastroenteritis. *Novartis Found. Symp.* **238**:82–96.
- Estes, M. K., and A. P. Morris. 1999. A viral enterotoxin. A new mechanism of virus-induced pathogenesis. *Adv. Exp. Med. Biol.* **473**:73–82.
- Farthing, M. J. 2000. Novel targets for the pharmacotherapy of diarrhoea: a view for the millennium. *J. Gastroenterol. Hepatol.* **15**(Suppl.):G38–G45.
- Field, M., and C. E. Semrad. 1993. Toxigenic diarrheas, congenital diarrheas, and cystic fibrosis: disorders of intestinal ion transport. *Annu. Rev. Physiol.* **55**:631–655.
- Fondacaro, J. D. 1986. Intestinal ion transport and diarrheal disease. *Am. J. Physiol.* **250**:G1–G8.
- Glass, R. I., J. Bresee, B. Jiang, J. Gentsch, T. Ando, R. Fankhauser, J. Noel, U. Parashar, B. Rosen, and S. S. Monroe. 2001. Gastroenteritis viruses: an overview. *Novartis Found. Symp.* **238**:5–19.
- Halaihel, N., V. Lievin, F. Alvarado, and M. Vasseur. 2000. Rotavirus infection impairs intestinal brush-border membrane Na⁺/solute cotransport activities in young rabbits. *Am. J. Physiol. Gastrointest. Liver Physiol.* **279**:G587–G596.
- Hamilton, J. R. 1988. Viral enteritis. *Pediatr. Clin. N. Am.* **35**:89–101.
- Hauser, H., K. Howell, R. M. Dawson, and D. E. Bowyer. 1980. Rabbit small intestinal brush border membrane preparation and lipid composition. *Biochim. Biophys. Acta* **602**:567–577.
- Holtug, K., M. B. Hansen, and E. Skadhauge. 1996. Experimental studies of intestinal ion and water transport. *Scand. J. Gastroenterol.* **216**(Suppl.):95–110.
- Hopfer, U., and C. M. Liedtke. 1987. Proton and bicarbonate transport mechanisms in the intestine. *Annu. Rev. Physiol.* **49**:51–67.
- Jourdan, N., J. P. Brunet, C. Sapin, A. Blais, J. Cotte-Laffitte, F. Forestier, A. M. Quero, G. Trugnan, and A. L. Servin. 1998. Rotavirus infection reduces sucrose-isomaltase expression in human intestinal epithelial cells by perturbing protein targeting and organization of microvillar cytoskeleton. *J. Virol.* **72**:7228–7236.
- Loo, D. D., T. Zeuthen, G. Chandy, and E. M. Wright. 1996. Cotransport of water by the Na⁺/glucose cotransporter. *Proc. Natl. Acad. Sci. USA* **93**:13367–13370.
- Lorrot, M., M. H. Cocconnier, and M. Vasseur. 2001. Rotavirus infection increases net chloride secretion by stimulating the Cl⁻/H⁺ symporter of young rabbit intestinal brush-border membrane. *J. Physiol. Biochem.* **57**:160.
- Lundgren, O., and L. Svensson. 2001. Pathogenesis of rotavirus diarrhea. *Microbes Infect.* **3**:1145–1156.
- Milanick, M. A., and R. B. Gunn. 1986. Proton inhibition of chloride exchange: asynchrony of band 3 proton and anion transport sites? *Am. J. Physiol.* **250**:C955–C969.
- Morris, A. P., and M. K. Estes. 2001. Microbes and microbial toxins: paradigms for microbial-mucosal interactions. VIII. Pathological consequences of rotavirus infection and its enterotoxin. *Am. J. Physiol. Gastrointest. Liver Physiol.* **281**:G303–G310.
- Orsenigo, M. N., M. Tosco, and A. Faelli. 1991. Cl⁻/HCO₃⁻ exchange in the basolateral membrane domain of rat jejunal enterocyte. *J. Membr. Biol.* **124**:13–19.
- Rossmann, H., S. L. Alper, M. Nader, Z. Wang, M. Gregor, and U. Seidler. 2000. Three 5'-variant mRNAs of anion exchanger AE2 in stomach and intestine of mouse, rabbit, and rat. *Ann. N.Y. Acad. Sci.* **915**:81–91.
- Snedecor, G. W., and W. G. Cochran. 1967. *Statistical methods*, 6th ed. Iowa State University Press, Ames, Iowa.
- Starkey, W. G., J. Collins, D. C. Candy, A. J. Spencer, M. P. Osborne, and J. Stephen. 1990. Transport of water and electrolytes by rotavirus-infected mouse intestine: a time course study. *J. Pediatr. Gastroenterol. Nutr.* **11**:254–260.
- Stephen, J. 2001. Pathogenesis of infectious diarrhea. *Can. J. Gastroenterol.* **15**:669–683.
- Touzani, K., F. Alvarado, and M. Vasseur. 1997. pH gradient effects on chloride transport across basolateral membrane vesicles from guinea-pig jejunum. *J. Physiol.* **500**:385–400.
- Touzani, K., M. Cauzac, M. Vasseur, and F. Alvarado. 1994. Rheogenic Cl⁻ conductance and Cl⁻/Cl⁻-exchange activities in guinea pig jejunal basolateral membrane vesicles. *Am. J. Physiol.* **266**:G271–G281.
- van Melle, G., and J. W. Robinson. 1981. A systematic approach to the analysis of intestinal transport kinetics. *J. Physiol. (Paris)* **77**:1011–1016.
- Vasseur, M., M. Cauzac, and F. Alvarado. 1989. Electroneutral, HCO₃⁻-independent, pH gradient-dependent uphill transport of Cl⁻ by ileal brush-border membrane vesicles. Possible role in the pathogenesis of chloridorrhea. *Biochem. J.* **263**:775–784.
- Vasseur, M., M. Cauzac, R. Frangne, and F. Alvarado. 1992. Trans-potassium effects on the chloride/proton symporter activity of guinea-pig ileal brush-border membrane vesicles. *Biochim. Biophys. Acta* **1107**:150–158.
- Vasseur, M., M. Cauzac, I. Garcia, and F. Alvarado. 1992. Chloride transport in control and cystic fibrosis human skin fibroblast membrane vesicles. *Biochim. Biophys. Acta* **1139**:41–48.
- Vasseur, M., M. Cauzac, K. Touzani, and F. Alvarado. 1989. Mechanisms of trans-chloride activation of a Cl⁻/H⁺ symport in brush-border membrane vesicles from guinea-pig ileum. *Biochem. Soc. Trans.* **17**:1004.
- Zhang, M., C. Q. Zeng, A. P. Morris, and M. K. Estes. 2000. A functional NSP4 enterotoxin peptide secreted from rotavirus-infected cells. *J. Virol.* **74**:11663–11670.